CONDENSATION OF OLEFINS ON CLAYS. GAS-SOLID SYSTEMS. PART I: GRAVIMETRIC METHODS

EDUARDO CHOREN, ALEXANDER MORONTA, GUSTAVO VARELA, ARNEDO ARTEAGA AND JORGE SÁNCHEZ

Centro de Superficies y Catálisis, Facultad de Ingeniería, Universidad del Zulia,
Apartado 15251, Maracaibo 4003A, Venezuela

Abstract—The adsorption-condensation of olefins was studied on 7 adsorbents: 2 commercial clays, a natural clay and its protonated form, γ-alumina and porous and nonporous silicas. These adsorbents were characterized by X-ray diffraction (XRD), chemical analysis, thermogravimetric analysis (TGA), differential thermal analysis (DTA) and determination of specific surface area measurement by the BET method. The experiments were carried out gravimetrically, in gas- or vapor-solid systems, at 25 °C, and on adsorbents dried at 120 °C. Adsorption-condensation of olefins are fast processes, diffusion controlled. Alumina and silicas adsorb olefins and paraffins only reversibly, but are unable to condense olefins. The water polarized by the countercations is the source of Brønsted acid sites. When the gas phase is evacuated or swept with inert gas, the condensation terminates. On clays, paraffins are reversibly adsorbed but no condensation was observed.

Key Words—Adsorption, Clays, Condensation, Olefins, Oligomerization, Paraffins.

INTRODUCTION

A benzene alkylation plant with hydrogen fluoride (HF) as catalyst encountered a problem with the final product, because it had a concentration of olefins above specification. The proposed solution was the selective adsorption of these olefins onto clays. A number of commercial clays were tested by percolating the impure product, in a column 0.8 cm in diameter by 10 cm long, packed in a glass tube. The results were excellent: an initial drop of the bromine number to a tenth or less and a high processing capacity. A stream of hot benzene and drying with warm air were enough to reactivate the clay. During the run, clays changed colors: greenish, brownish and finally a black front started at the top of the column and descended until all of the column turned black. The activity remained for some time until the Br number marked the end of the run.

All of these effects have been described in numerous papers on clays exchanged with salts of all the metal groups, or organic complexes of them, or pillared clays, published during the last 30 years. But few of those papers addressed the reactions of olefins in the range 20–25 °C on clays dried at 120 °C.

The aim of this study is to identify and evaluate the different factors and steps in olefin adsorption-condensation processes using vapor-solid or gas-solid systems. "Condensation", in this work, involves all of the reactions that generate products of higher molecular weight, such as etherifications and oligomerization.

EXPERIMENTAL

Adsorbates

Adsorbates were propylene, Scott, >99.5%; 1-butene, Matheson, >99.0%; *cis*-2-butene, Linde, >99.0%; cyclohexane, Baker, >98.0%; cyclohexene, Baker, B.P. 82–84 °C; 2,2-dimethylbutane, Fluka, >99.0%; and 2,3-dimethyl-2-butene, Fluka, >99.5%. All liquid adsorbates were purified by the freezing-thaw method before adsorption.

Adsorbents

Adsorbents were:

1) Two similar commercial activated clays from Filtrol-Harshaw, Filtrol 24 (F24) and Filtrol 124 (F124).

2) A Venezuelan clay (T1) from Tinaquillo, State of Cojedes, purified as described in Choren et al. (1996).

3) A protonated form of the T1 clay (T1H), prepared by treatment with a hot NH_4NO_3 solution, 1.5 M as indicated by Lunsford (1968). The derivative clay was washed with distilled water, dried and heated to 300 °C to decompose the salt. The very small variation in the MgO content of this clay (Table 1) suggests that Mg is a structural component and not a free ion.

4) Cabosil, a high-purity silica aerogel from Cabot, Inc. The particles of Cabosil are nonporous spheres with homogeneous radii. High-purity γ-alumina from Rhône-Poulenc, G.F.S.C. High-purity silica-gel, Baker Reagent, 60–200 mesh.

All of the adsorbents were ground to pass through a 200 sieve. The pretreatments are indicated herein.

X-ray powder diffraction traces of the clays were potentiometrically recorded using a Philips PW-1720 diffractometer with Co anode. The chemical composition of clays was determined by atomic absorption and emission spectroscopies and conventional chemical analysis.

The TGA was carried out in a Cahn D-200 electrobalance. Samples of 100–150 mg were subjected to a heating program (β = 10 °C/min) in a He flow (30–

213

Table 1. Clays' chemical composition.

Clay	SiO₂	Al₂O₃	Na₂O	CaO	MgO	K₂O	Fe₂O₃	SO₃	Si/Al
F24	66.4	10.2	0.1	0.1	2.6	0.1	0.8	1.2	5.9
F124	67.2	8.8	0.1	0.1	2.7	0.1	0.7	1.3	5.5
T1	57.6	18.3	0.9	0.08	1.3	ND	21.8	ND	2.7
T1H	61.2	16.0	Tr	Tr	1.1	ND	20.5	ND	3.3

ND: Not determined; Tr: traces.

40 SPT mL/min). Masses and the first derivative thermograms were plotted directly after each run. The DTA diagrams were obtained using TA Instruments equipment. Samples of 7–8 mg were heated at 10 °C/min, sweeping the furnace with He (30 STP mL/min). Temperatures were calibrated with In and Ag as standards.

The specific area of the samples, previously dried for 2 h at 200 °C, was measured by the BET method with UHP nitrogen in a Cahn RG-HV electrobalance coupled to a vacuum line that was allowed to reach 10^{-2} Pa.

Hydrocarbon Adsorption

Hydrocarbon adsorption was measured gravimetrically in the Cahn D-200 electrobalance. The standard procedure was the following: 100–150 mg of adsorbent were dried for 2 h at 120 °C at a pressure of 0.1 Pa to take the initial mass. Then the hydrocarbon was admitted until the pressure reached 2.5 kPa. This pressure was maintained for 2 h, while the mass was continuously recorded. The total adsorbed amount (Ta, mmol/g) is the difference between the sample mass in equilibrium with the gas phase at this time and the initial mass standardized to 1 g of adsorbent. After 0.5 h of evacuation, the final mass was recorded and the irreversibly adsorbed amount (IA, mmol/g) was calculated. In several cases the pretreatment, the equilibrium pressure or the time of adsorption was changed as indicated herein.

RESULTS AND DISCUSSION

Chemical Composition

Table 1 shows the chemical composition of the 4 clays studied. The high Si/Al ratio for the F24 and F124 clays may be the result of the activation method that, given the SO₃ content, has been leaching with sulfuric acid. It is known that acid treatment dissolves Al from tetrahedral positions (Little 1966). The T1H has increased its Si/Al ratio with respect to that of its parent T1, notwithstanding the fact that NH₄⁺ is a weak acid.

Structures

Figure 1 shows the clays' X-ray powder diffractograms. The F24 and F124 clay diffractograms show peaks corresponding to smectites with some quartz im-
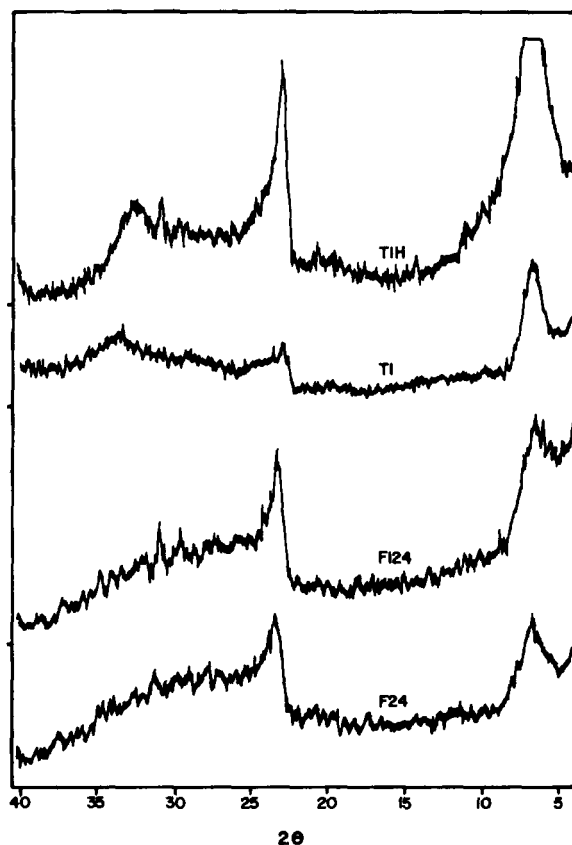

Figure 1. Clays' X-ray powder diffractograms.

purities. The T1 XRD looked like a consistent smectite (Grim and Kulbicki 1961).

Table 2 shows the d(001) spacing of the 4 clays. Those of F24 and F124 clays appear to be too wide, in spite of their low metal cation content; but again, the drastic interbasal spacing increase in T1H shows the same trend.

Thermogravimetric Analysis (TGA)

All of the clay samples showed similar TGA diagrams. A typical thermogram is shown in Figure 2, which includes the integral and first derivative curves. The integral curve shows 2 regions with negative slope, nearly linear. The first region, at lower temperatures, is about 1 order of magnitude steeper than the other. It corresponds to the loss of hygroscopic water, and reaches a maximum slope at 100–120 °C. The

Table 2. The d(001) spacing of clays.

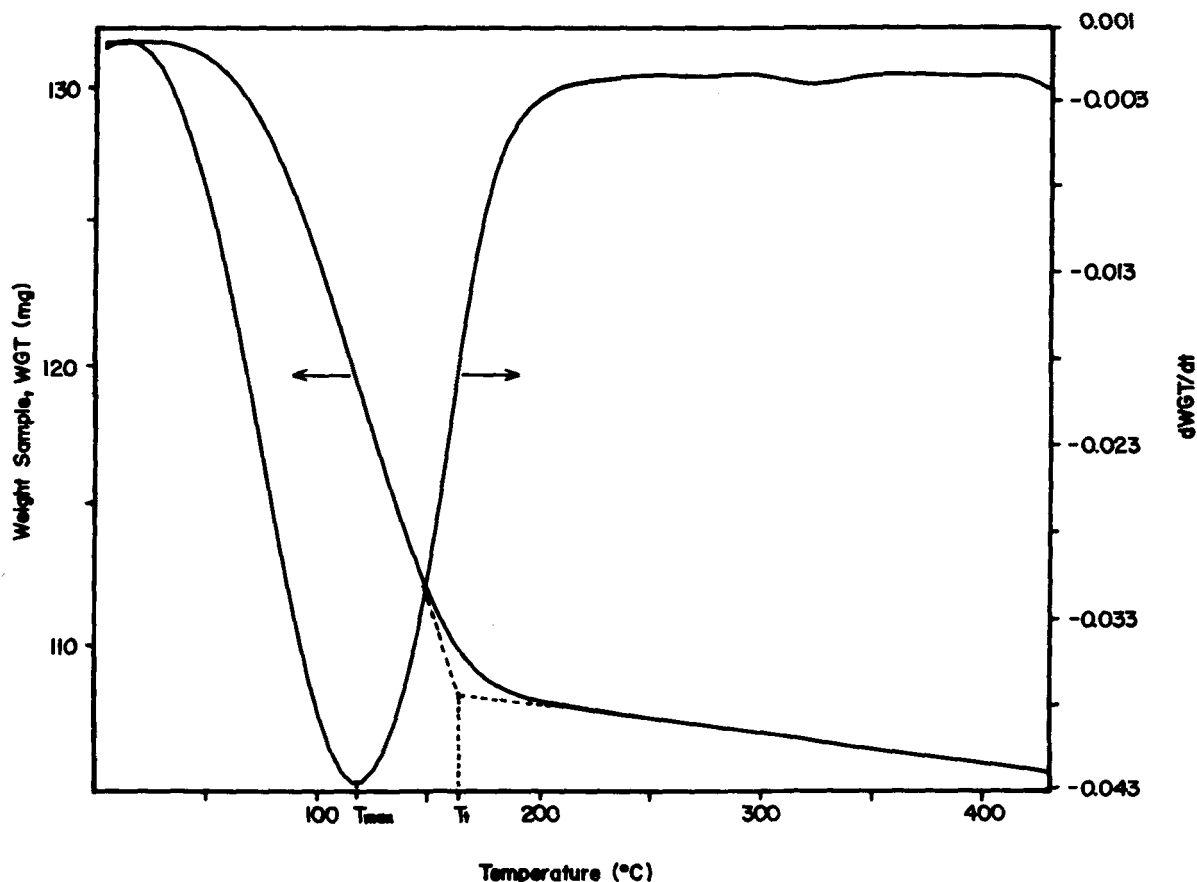| Clay	d(001) (Å)
F24	15.3
F124	16.6
T1	15.8
T1H	15.4

Figure 2. Typical thermogram of a clay. Key: Tmax = temperature of maximum water loss rate, and Tt = transition temperature.

second region of the curve, much slower, is associated with both the loss of strongly adsorbed water and the reaction between vicinal and geminal hydroxyls. To obtain a rough picture of the water distribution in the clays, both parts of the integral curve were extrapolated linearly. The cross point was arbitrarily designated as the transition temperature (Tt). The mass lost until that temperature was considered to be hygroscopic water (Wh) and the remainder as structural water (Ws). The temperature of maximum slope (Tmax)

was identified by the minimum in the derivative curve. As the TGA runs ended at 500 °C, the total water (Wt) was determined in samples heated in a vacuum at 800 °C until constant weight in a quartz tube. The surface coverage (θ) was calculated on the basis of the hygroscopic water, by conservatively estimating the water molecule area in 10 $\mathring{A}^2$ and the BET specific surface area. As the dehydration for 2 h at 120 °C produces a loss of water greater than the one corresponding to Tt in the graph, the eighth column (θ_{120}) reports the water present in the clay immediately before the adsorption of the hydrocarbon. These values are reported in Table 3.

Differential Thermal Analysis (DTA)

Figure 3 shows the DTA diagrams of F124, T1 and T1H samples. All clays showed similar thermal behavior until 1000 °C. The first endotherm, corresponding to loss of hygroscopic water in the DTA, is 30–40 degrees lower than that obtained by TGA. Table 4 lists these differences. This is a mass effect: while 100–150 mg are used in each run of TGA, only 6–8 mg are enough for a DTA run. These differences have
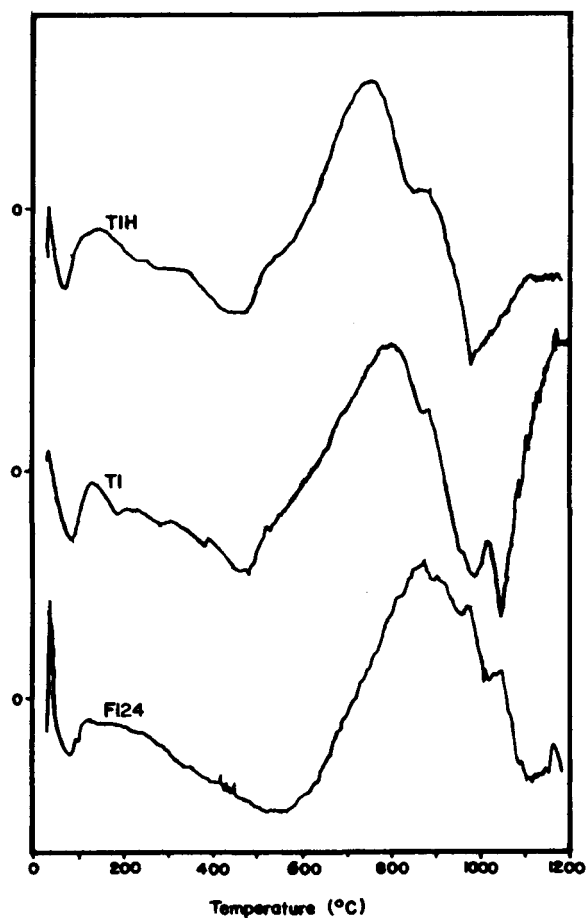
Table 3. Water distribution in clays. Key: Tmax = temperature of maximum water loss rate, Tt = transition temperature, Wt = total water, Wh = hygroscopic water, Ws = structural water, θ = surface coverage and θ_{120} = coverage degree corresponding to the water present in the clay immediately before the adsorption of the hydrocarbon.

Clay	Tmax °C	Tt °C	Wt %	Wh %	Ws %	θ	θ_{120}
F24	125	170	21.6	16.7	4.9	1.7	1.0
F124	125	170	25.4	16.1	9.3	1.6	0.9
T1	125	185	21.5	15.1	6.4	7.7	4.1
T1H	107	140	11.4	5.4	6.0	0.7	0.1

Figure 3.   DTA diagram of F124, T1 and T1H clays.

Table 4.   Differences between the temperatures of maximum rate of water loss obtained by TGA and DTA.

Clay	TGA (°C)	DTA (°C)
F124	125	86
T1	125	90
T1H	107	75

mass during the adsorption of cyclohexane and cyclohexene. At 10–15 min, the adsorbed paraffin is in equilibrium with the gas phase; afterward, the solid ceases to take gas and the mass remains constant. The adsorption of paraffins is totally physical in nature, because after evacuation the mass of the adsorbent remains identical with the initial mass. Paraffins give isotherms of type II and can be used, when the area per molecule is known, to calculate the accessible specific surface area (Gonzo 1982). For olefins, on the contrary, the fast step is followed by a slow, nearly linear uptake for at least 2 h. The inset in Figure 4 shows that, as expected, lower temperatures increase the adsorbed mass for paraffins and alkenes. Table 6 makes the picture clearer. The amount of total adsorption decreases when the temperature increases, but condensation, an activated process, increases. In this table, for the adsorbed cyclohexene, the difference between the total amount and that of cyclohexane is equal to the irreversible fraction of the cyclohexene at the same temperature, suggesting that the sites for reversible and irreversible adsorption are not the same.

The specific surface areas (SA) and the 1-butene uptakes for the 7 adsorbents studied are listed in Table 7. It is evident that the pure silicas are not active for condensation in the experimental conditions and that the activity of alumina is too low to be considered significant. The comparison between the values of T1 and T1H clays is interesting: while the second has a

been explained by Schilling (1990) and are associated with diffusional effects depending upon the amount and compactness of the sample. This effect does not invalidate the qualitative results of TGA, although the temperatures from the DTA are the most exact. The intense exotherm that is extended from 600 to about 1000 °C was associated with a clay crystalline reordering by contraction of the greater interplanar distances. To corroborate this hypothesis, a sample of T1H was heated at 800 and 1100 °C and observed by XRD. Table 5 shows the relevant XRD peaks. The I/Io values have comparative purposes only: the value of 100 was assigned to the higher peak and the others were evaluated proportionally. The sample calcinated at 800 °C for 2 h shows an appreciable reduction of the interbasal spacing. Heating of 1100 °C causes the disappearance of the spacings greater than 3 Å. Considering that these processes occur in solid phase, the results do not correspond to equilibrium values but are enough to prove the supposition correct.

Table 5.   Spacings of T1H in equilibrium with atmospheric moisture, heated at 800 °C and at 1100 °C.

2θ	d (Å)	I/Io
T1H		
6.6	15.4	100
22.8	4.52	30
33.2	3.13	30
T1H-800		
10.8	9.5	100
23.2	4.45	70
32.8	3.17	75
39.0	2.69	30
41.8	2.50	30
T1H-1100		
35.7	2.93	45
38.6	2.70	30
42.2	2.49	100
51.5	1.14	30

Hydrocarbon Adsorption

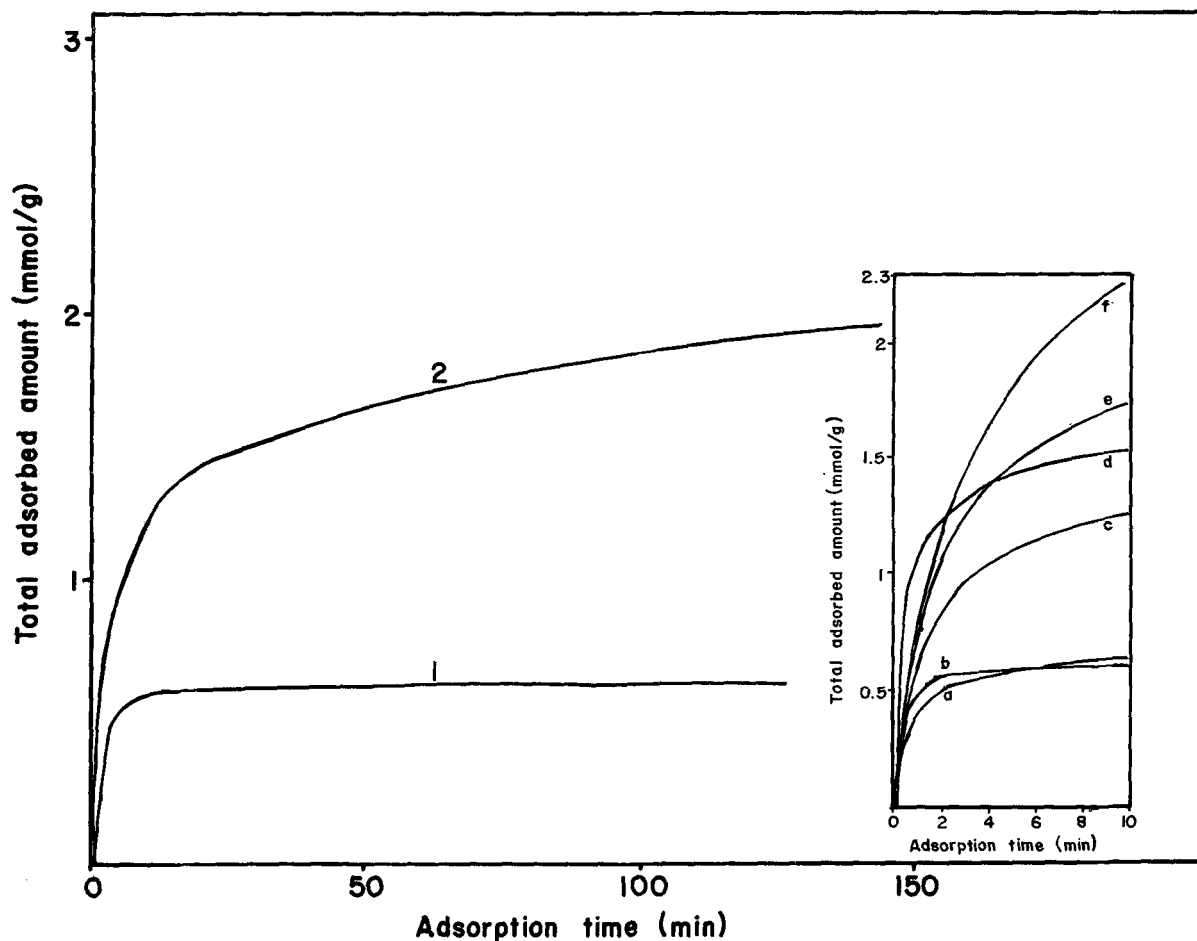Both chemisorption and condensation of hydrocarbons are fast reactions. Figure 4 shows the adsorbed

Figure 4. Gravimetric measurement of cyclohexane (1) and cyclohexene (2) adsorption on F24 clay. Inset: a) cyclohexane, 25 °C; b) methylcyclopentane, 25 °C; c) cyclohexene, 25 °C; d) methylcyclopentane, 0 °C; e) cyclohexane, 0 °C; f) cyclohexene, 0 ° C.

surface area 4 times greater and an interbasal spacing more than 50% (Table 2) greater than its parent, the amounts of adsorbed olefin remained identical. The activity of a clay is determined by 3 factors: the surface density of active sites, the accessibility of the internal area to the reactant molecule and the availability of sufficient space to allow an additional monomer to reach the reaction site with the adequate angle for condensation to take place.

To obtain more information about the role of internal and external surfaces in the condensation of olefins, a bulky paraffin, 2,2-dimethylbutane (DMB) and an olefin, 2,3-dimethyl-2-butene (D2B) were adsorbed onto 2 samples of F124 clay pretreated for 2 h in a

Table 6. Adsorption of cyclohexane and cyclohexene (mmol/g) on F24 clay, $t = 10$ min, at 25 °C and 0 °C, $p = 2.5$ kPa.

Adsorbate	Temperature °C	TA mmol/g	IA mmol/g
Cyclohexene	25	1.253	0.69
	0	2.236	0.42
Cyclohexane	25	0.650	0.00
	0	1.718	0.00

TA: Total adsorbed amount; IA: irreversibly adsorbed amount.

Table 7. Specific areas (SA) and 1-butene adsorption on 7 adsorbents dried at 120 °C 2 h at 25 °C and 2.5 kPa. Key: TA = Total Adsorption, IA = Irreversible Adsorption.

Sample	TA mmol/g	IA mmol/g	SA m²/g
F24	1.03	0.85	337
F124	1.18	0.98	332
T1	0.35	0.34	65
T1H	0.37	0.33	257
Cabosil	0.04	0	250
SiO_2	0.12	0	256
γ-Al_2O_3	0.23	0.05	226

Table 8. Amounts adsorbed, in mmol/g, 2 h at 25 °C and a pressure of 2.5 kPa, of 2,2-dimethylbutane (DMB) and 2,3 dimethyl-2-butene (D2B) on F124 clay preheated at 120 °C and 800 °C.

Pretreat. t °C	TA DMB	TA D2B	IA D2B	SBET m²/g	IA/TA D2B
120	0.42	3.28	2.25	332	0.69
800	0.28	1.92	0.77	89	0.40
Δ%	−33.3	−40.5	−65.8	−73.2	−42.0

vacuum at 120 and 800 °C. The adsorption of DMB is associated with the surface accessibility. The amount of D2B adsorbed is determined by the 3 factors enumerated in the preceding paragraph. Table 8 suggests some interesting observations. The small drop in the DMB adsorption compared with that of nitrogen indicates that DMB always has a limited access to the interlamellar spacing. The last column indicates the fraction of the total adsorbed amount of D2B that has condensed. The 42% decrease in this fraction is an effect of the destruction of active sites and space availability. Although the D2B molecule is flat and rigid due to the sp² character of the 2 central carbon atoms, and is less hindered than DMB from penetrating the interlamellar spacing, the restriction still exists, as shown by the smaller decrease in total adsorption compared with that of nitrogen (last row). Therefore, it is reasonable to suppose that the loss of activity is more a consequence of the destruction of active sites than of space availability. In 2 simultaneous papers on the adsorption kinetics of methanol, 2-propanol and *t*-butanol (Breen et al. 1987a) and tetrahydrofuran, tetrahydropyran and 1,4-dioxan (Breen et al. 1987b) on trivalent metal-exchanged montmorillonite, it was shown that the rates of adsorption increased as the sample and grain size decreased, indicating that inter- rather than intraparticle mass transfer was the rate-limiting process. The authors showed that the bed volume and the particle size variations have a greater effect on adsorption than the pretreatment temperature.

The concept of space availability deserves some comments. As an example, Tennakoon et al. (1983) found, in 2 separate experiments, that *n*-pentanol and isobutene intercalate in smectites. Thus, they induced that these molecules react in the same place to give principally 1:1 dipentyl-ether for *n*-pentanol and methyl-*tert*-butyl ether (MTBE) (with methanol) for isobutene. In a closed vessel at 180 °C for 3 h, 45% of the pentanol dehydrated to produce mainly 1:1 ether. However, when nitrogen saturated with pentanol was passed over the heated clay, the only significant product was pentene. In further experiments, the dehydration was conducted in a high-pressure arrangement and, again, when the clay was placed in the vapor-phase, the product was pentene, and when the clay was submerged in the liquid phase, it yielded ether. They concluded that the principal reason was that the liquid leached the products that blocked the active sites, but in the vapor-solid reactions these remained on the site. Figure 5 shows a scheme of MTBE in which the geometry was optimized and the energy minimized by applying the Pollak-Rivière method. The figures represent selected internuclear distances. The distance between the H in positions A and B is 4.30 Å. If the van der Waals radius of hydrogen is added, the smaller dimension of the MTBE molecule is 6.70 Å. The interbasal spacing measured by Tennakoon et al. (1983) during the reaction was 14 Å; if the thickness of the lamellae is discounted, the free space between them is 5–6 Å.

The MTBE molecule is dimensionally similar to 2,2-dimethylbutane. As shown in Table 8, the access
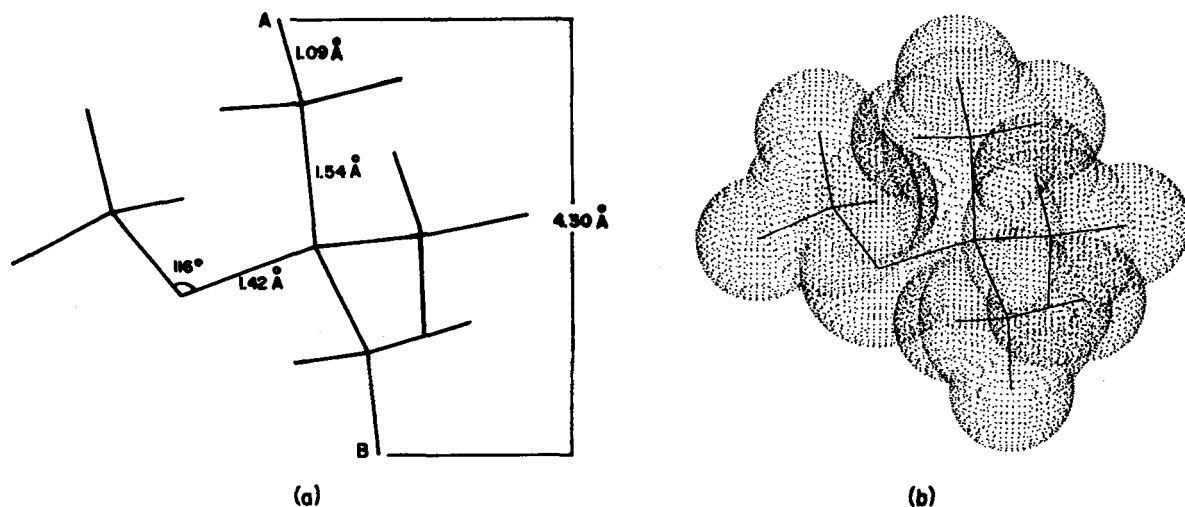
(a)

(b)

Figure 5.   Molecule of methyl-*tert*-butyl ether: a) internuclear distances, and b) van der Waals molecule.

Table 9. Room temperature adsorption of cyclohexene and 1-butene on F24 clay dried at 120 °C.

Time	10 min				120 min			
	TA mmol/g	IA mmol/g	P kPa	IA/TA	TA mmol/g	IA mmol/g	P kPa	IA/TA
Cyclohexene	1.25	0.69	1.48	0.55	1.95	1.15	1.61	0.59
1-butene	0.76	0.58	3.06	0.76	1.03	0.85	2.5	0.82

of 2,2-dimethylbutane to the interlayer spaces is, at least, very limited. If the apparent difference in selectivity had its origin in space availability it would be the opposite, because olefins are smaller molecules than ethers. The XRD evidences of Tennakoon et al. (1983) seem to show the intercalation of molecules of alcohol and olefins, but this does not imply that the reaction occurs in the same place. Given that the clay is finally grounded, the nuclear magnetic resonance (NMR) signals could not discriminate between internal and external surfaces.

Without definitive evidence about the participation of the internal clay surface in this reaction, the difference in concentrations betwen experiments appears to be the most important factor: in the Tennakoon et al. (1983) experimental conditions, the concentration in the liquid phase is more than 2 orders of magnitude greater than in the vapor phase.

Although no systematic kinetics study of condensation was performed in this work, the adsorption of 2 olefins, 1 terminal and 1 cyclical, was carried out for 10 and 120 min on F24 clay. Table 9 shows some interesting regularities. The ratio of the fraction condensed at 10 min is similar to that found at 120 min; the differences are below the experimental error.

An intent to produce mixed chains led to finding an unexpected aspect of the process. Samples of F24 clay were put in contact with a given olefin following the standard gravimetric adsorption procedure. After a certain time, the system was evacuated and another olefin was admitted into it. The increasing preadsorbed amounts of the first olefin were regulated by controlling pressure and time (always at 25 °C). Table 10

Table 10. Amounts of the blocking olefin (gas 1), and the probe olefin (gas 2) for room temperature adsorption of cyclohexene and 1-butene on F24 clay dried at 120 °C.

Gas 1 mmol/g	Gas 2		Pressure
	TA mmol/g	IA mmol/g	
Cyclohexene	1-Butene		kPa
0.00	0.759	0.577	3.06
0.538	0.218	0.000	3.08
1-Butene	Cyclohexene		
0.000	1.253	0.690	1.48
0.577	1.020	0.256	1.49
1.100	0.761	0.038	1.49
1.434	0.593	0.000	1.52

presents typical results: Gas 1 is the preadsorbed gas, and Gas 2 is the probe gas adsorbed for 10 min. The amounts are expressed in mmol/g of clay and the pressures in kPa. Several remarks may be drawn from Table 10. The most interesting of these is that when the system is evacuated, the heterogeneous acidic catalytic condensation comes to an end and the product remains on the surface, blocking the active sites. The most plausible explanation may be a physical blocking of sites. A real termination implies the liberation of active sites to react with a new monomer, or the formation of an ester with the surface (Stevens 1975), but the oligomers are leachable with solvents that exclude a covalent oligomer-clay bond. That is perhaps the reason why Vogel et al. (1990) found that isobutene does not react after the flow of hydrocarbon was switched off after 1 h of adsorption at 30 °C.

The gravimetric adsorption measurements are not sufficient to give a complete picture of the process of olefin adsorption-condensation on clays at room temperature, but they serve as a basis for a set of preliminary remarks. Adsorption-condensation of olefins are fast processes. Alumina and silica adsorb olefins reversibly but are unable to condense them. When Si and Al are together in the crystal network, the required countercations are the true source of the active Brønsted acid sites. Mortland et al. (1963), and Tarasevich (1988) agree in considering that the structural hydroxyls in montmorillonites are relatively inactive at room temperature and that the Brønsted sites are associated with the water molecules in the cation coordination sphere. The condensation process terminates when the gas phase is evacuated or swept with an inert gas. Paraffins are reversibly adsorbed on the 7 adsorbents studied here, but no condensation was observed in any of them.

REFERENCES

Breen C, Deane AT, Flynn JJ. 1987a. Vapor-phase sorption kinetics for methanol, propan-2-ol, and 2-methyl propan-2-ol on Al^{3+}-, Cr^{3+}-, and Fe^{3+}-exchanged montmorillonite. Clays Clay Miner 35:336–342.

Breen C, Deane AT, Flynn JJ. 1987b. Vapor-phase sorption kinetics for tetrahydrofuran, tetrahydropyran, and 1,4-dioxan by Al^{3+}- and Cr^{3+}-exchanged montmorillonite. Clays Clay Miner 35:343–346.

Choren E, Moronta A, Huerta L, Meyer A. 1996. Comparative study of a Venezuelan clay. Rev Téc Ing Univ Zulia 19.2:107–118.

Gonzo EE. 1982. A rapid and accurate gravimetric technique for measuring the specific surface areas of porous solids. Appl Catal 2:359–362.

Grim RE, Kulbicki G. 1961. Montmorillonite: High temperature reactions and classification. Am Mineral 46:1329–1368.

Little LH. 1966. Infrared spectra of adsorbed species. London: Academic Pr. 345 p.

Lunsford JH. 1968. Surface interactions of NaY and decationated Y zeolites with nitric oxide as determined by electron paramagnetic resonance spectroscopy. J Phys Chem 72:4163–4168.

Mortland MM, Fripiat JJ, Chaussidon J, Uytterhoeven J. 1963. Interaction between ammonia and the expanding lattices of montmorillonite and vermiculite. J Phys Chem 67:248–258.

Schilling MR. 1990. Effects of sample size and packing in the thermogravimetric analysis of calcium montmorillonite Stx-1. Clays Clay Miner 38:556–558.

Stevens MP. 1975. Polymer chemistry: An introduction. Reading, MA: Addison-Wesley. p 137–139.

Tarasevich YI. 1988. Acidic properties of water bound to the surfaces of mineral ion-exchangers. Theor Eksp Khim 24:590–598 (in Russian). CA 110. 293333m.

Tennakoon DTB, Schlögl R, Rayment T, Klinowski J, Jones W, Thomas JM. 1983. The characterization of clay-organic systems. Clay Miner 18:357–371.

Vogel AP, O'Connor CT, Kojima M. 1990. Thermogravimetric analysis of the iso-butene oligomerization activity of various forms of synthetic mica-montmorillonite. Clay Miner 25:355–362.